

Quark structure of isoscalar- and isovector-scalar mesons and nuclear matter property

Yao Ma^{1,2,*} and Yong-Liang Ma^{3,1,4,†}

¹*School of Fundamental Physics and Mathematical Sciences,
Hangzhou Institute for Advanced Study, UCAS, Hangzhou, 310024, China*

²*University of Chinese Academy of Sciences, Beijing 100049, China*

³*Nanjing University, Suzhou, 215163, China*

⁴*International Center for Theoretical Physics Asia-Pacific (ICTP-AP), UCAS, Beijing, 100190, China*



(Received 26 November 2023; accepted 21 March 2024; published 16 April 2024)

It was found that isoscalar-scalar and isovector-scalar mesons play significant roles in nuclear matter physics. However, the underlying structures of these resonances are not yet well understood. We construct a three-flavor baryonic extended linear sigma model including both the two- and four-quark constituents of scalar mesons with respect to the axial transformation and study the nuclear matter properties with the relativistic mean field method. The nuclear matter properties at saturation density and hadron spectra are well reproduced with this model simultaneously, and only the two-quark component of the scalar mesons couples to baryon fields and dominates the nuclear force. A plateau-like structure is found in the symmetry energy of nuclear matter due to the multimeson couplings, and it is crucial for understanding the neutron skin thickness of ^{208}Pb and the tidal deformation of neutron star from GW170817. At high-density regions, vector mesons are found to be rather crucial, especially the ones coupling with four-quark configurations. This model can be easily extended to study neutron stars, even with hyperons in their interior.

DOI: [10.1103/PhysRevD.109.074022](https://doi.org/10.1103/PhysRevD.109.074022)

I. INTRODUCTION

Nuclear matter (NM) is a kind of strongly interacting system which is mainly composed of nucleons and mesons and, maybe, other novel structures (see, e.g., Refs. [1–4] for reviews). Since NM is in the nonperturbative region of QCD which is not yet fully understood so far, many properties are still under debate.

Finite nuclei as well as infinite NM at low densities can be fairly well accessed by nuclear chiral effective field theories, pionless or pionful, anchored on some symmetries and invariances of QCD. However, these theories break at high densities relevant to the interiors of massive stars [2], and the higher-order expansion of the power counting and hadron resonances such as the lightest isoscalar-scalar meson (σ) and lowest-lying vector mesons are indispensable; see, e.g., Refs. [5–7], where the σ meson is regarded as the Nambu-Goldstone boson of scale symmetry breaking [8,9] and the vector mesons are included through the hidden local symmetry approach [10–12].

In the relativistic mean field (RMF) approach to NM, it has long been recognized that both the isoscalar-scalar mesons and the isovector-scalar mesons are crucial for obtaining the NM properties around the saturation density

$n_0 \approx 0.16 \text{ fm}^{-3}$, for example, the binding energy of nucleon e_0 due to the competition between the attractive force from σ meson and repulsive force from the ω meson [1,13,14]. The three- and four-point interactions of the sigma meson reduce the nuclear incompressibility [15], and the six-point interaction reproduces the properties of NM [16]. The interaction between sigma and vector mesons is also significant: The σ and ω meson coupling has been introduced to obtain a reasonable value of incompressibility coefficient K_0 [15,17]; the interactions between (σ) and ρ meson are crucial for describing the isospin asymmetric NM [1,13,14,18] and the neutron skin thickness of heavy nuclei ^{208}Pb [19,20].

In addition to the isoscalar-scalar meson, the isovector-scalar mesons δ [denoted as $a_0(980)$ in particle physics] should also be included in the RMF approach to NM, especially for asymmetric NM at high densities [21–24]. Recently, it has found that isoscalar- and isovector-scalar meson couplings are closely related to the stiffness of the equation of state (EOS) of NM and, therefore, the properties of neutron stars [25–28].

The existing studies have already shown that meson resonances heavier than the pion should be seriously considered in the study of nuclear matter, especially for asymmetric matter at high densities. However, these studies are considered separately, and the results are highly model dependent. So it is very interesting to construct a

* mayao@ucas.ac.cn

† ylma@nju.edu.cn

self-consistent model including σ , δ [following the convention of particle physics, we denote δ as $a_0(980)$ in the rest of this work] and ω , ρ , in addition to π , to study these resonance effects in a systematical way.

A systematic study of the scalar meson effects on NM is not so easy if one wants to concern more underlying dynamics of QCD, since, unlike pions, scalar mesons cannot be regarded as Nambu-Goldstone bosons of chiral symmetry breaking, and their quark contents still puzzle physicists [29]. Considering their mass ordering, it is very difficult to arrange scalar mesons below 1 GeV as pure $q\bar{q}$ states, and the four-quark components of scalar mesons should be taken into account. The purpose of this work is to investigate the effects of the quark contents of scalar mesons on NM properties.

To consider the two- and four-quark contents in the model, we follow the idea of Refs. [30–33], where an extended linear sigma model (ELSM) with both the two-quark and four-quark configurations was included and the physical states—the mixing states of the two- and four-quark configurations—were obtained by fitting the data [34–37]. We couple the scalar meson states to baryons with respect to the axial symmetry [38,39]. Since the two- and four-quark components have different axial transformations, the quark contents of the scalar mesons affect the properties of NM. In addition to the scalar mesons, the vector mesons are introduced as chiral representations with two-quark configurations [40].

By taking the RMF approximation using such constructed baryonic ELSM (bELSM), we found that both scalar mesons and vector mesons contribute to the EOS, and the quark contents of the scalar mesons also affect the EOS in a sizable way, especially at high-density regions. A plateaulike structure of symmetry energy is found around saturation density $n_0 \approx 0.16 \text{ fm}^{-3}$, which is the key to understand the neutron skin of ^{208}Pb and tidal deformability of neutron stars. Another interesting finding is $|g_{\sigma NN}| \sim 10$ and $|g_{\omega NN}| \sim 13$, which is consistent with the results from other approaches [28,41,42].

This paper is organized as follows: In Sec. II, we discuss the theoretical framework that will be used. The numerical results are discussed in detail in Sec. III. Our summary and perspective are given in the last section, and the Lagrangian of the three- and four-meson couplings are listed in the Appendix.

II. EXTENDED LINEAR SIGMA MODEL WITH BARYON FIELDS

We consider two three-flavor meson nonets Φ and $\hat{\Phi}$, which represent two-quark configuration $q\bar{q}$ and four-quark configuration $(qq)(\bar{q}\bar{q})$, respectively. Under chiral transformation, they transform as [31–33]

$$\Phi \rightarrow g_L \Phi g_R^\dagger, \quad \hat{\Phi} \rightarrow g_L \hat{\Phi} g_R^\dagger, \quad (1)$$

where $g_{L,R} \in \text{SU}(3)_{L,R}$. In addition, they transform under $(\text{U}(1))_A$ axial transformation as

$$\Phi \rightarrow e^{2i\nu} \Phi, \quad \hat{\Phi} \rightarrow e^{-4i\nu} \hat{\Phi} \quad (2)$$

with ν being the phase angle.

In the ELSM, we introduce the vector meson fields as current operators L_μ and R_μ with $\bar{q}_L \gamma_\mu q_L$ and $\bar{q}_R \gamma_\mu q_R$ configurations, respectively [40]. Under chiral transformation, they transform as

$$L_\mu \rightarrow g_L L_\mu g_L^\dagger, \quad R_\mu \rightarrow g_R R_\mu g_R^\dagger. \quad (3)$$

Considering the baryon as a three-quark configuration, we apply the diquark model for simplicity [38,39]. Then the baryon states are donated as $N_R^{(RR)}$, $N_L^{(RR)}$, $N_L^{(LL)}$, and $N_R^{(LL)}$, where (RR) and (LL) denote right- and left-hand diquark configurations, respectively, and R and L represent the quark configurations. Their transformation behaviors are given by

$$\begin{aligned} N_R^{(RR)} &\rightarrow g_R N_R^{(RR)} g_R^\dagger, & N_L^{(RR)} &\rightarrow g_L N_L^{(RR)} g_R^\dagger, \\ N_R^{(LL)} &\rightarrow g_R N_R^{(LL)} g_L^\dagger, & N_L^{(LL)} &\rightarrow g_L N_L^{(LL)} g_L^\dagger, \end{aligned} \quad (4)$$

and

$$\begin{aligned} N_R^{(RR)} &\rightarrow e^{-3i\nu} N_R^{(RR)}, & N_L^{(RR)} &\rightarrow e^{-i\nu} N_L^{(RR)}, \\ N_R^{(LL)} &\rightarrow e^{i\nu} N_R^{(LL)}, & N_L^{(LL)} &\rightarrow e^{3i\nu} N_L^{(LL)}. \end{aligned} \quad (5)$$

Since, in the effective model based on the linear realization of the chiral symmetry to be used here, there is no self-consistent power-counting mechanism, like the derivative expansion in chiral perturbation theory, we set the following counting rules to truncate our model:

- (I) The order of an effective term is determined by the number of valence quarks N_q .
- (II) Double trace terms are neglected because of large N_c suppression [43].
- (III) The terms containing vector mesons should be given priority considering rule I.

A. The Lagrangian

After the above discussion on the transformation properties of the meson and baryon fields, we are ready to construct the effective model. Formally, we decompose the Lagrangian of the bELSM as

$$\mathcal{L} = \mathcal{L}_M + \mathcal{L}_V + \mathcal{L}_B. \quad (6)$$

The \mathcal{L}_M is the gauged scalar and pseudoscalar part of ELSM which takes the form

$$\mathcal{L}_M = \frac{1}{2} \text{Tr}(D_\mu \Phi D^\mu \Phi^\dagger) + \frac{1}{2} \text{Tr}(D_\mu \hat{\Phi} D^\mu \hat{\Phi}^\dagger) - V_0(\Phi, \hat{\Phi}) - V_{\text{SB}}, \quad (7)$$

where $D_\mu \Phi = \partial_\mu \Phi - ig_1(L_\mu \Phi - \Phi R_\mu)$. V_{SB} stands for the effect of the explicit symmetry breaking, which will not be considered in this work. The interaction potential V_0 is given by

$$\begin{aligned} V_0 = & -c_2 \text{Tr}(\Phi \Phi^\dagger) + c_4 \text{Tr}(\Phi \Phi^\dagger \Phi \Phi^\dagger) + d_2 \text{Tr}(\hat{\Phi} \hat{\Phi}^\dagger) + e_3 (\epsilon_{abc} \epsilon^{def} \Phi_d^a \Phi_e^b \hat{\Phi}_f^c + \text{H.c.}) \\ & + c_3 \left[\gamma_1 \ln \left(\frac{\det \Phi}{\det \Phi^\dagger} \right) + (1 - \gamma_1) \ln \left(\frac{\text{Tr}(\Phi \Phi^\dagger)}{\text{Tr}(\hat{\Phi} \hat{\Phi}^\dagger)} \right) \right]^2, \end{aligned} \quad (8)$$

where the c_3 term accounts for the $U(1)_A$ anomaly of QCD [31,44,45] and the other terms are chiral invariant. It was found that the e_3 terms are crucial for scalar meson mass split between octet and singlet [46].

By considering the transformation properties (3), the chiral and axial invariant Lagrangian for the vector meson part at the lowest order takes the form

$$\begin{aligned} \mathcal{L}_V = & -\frac{1}{4} \text{Tr}(R_{\mu\nu}^2 + L_{\mu\nu}^2) + i \frac{g_2}{2} \{ \text{Tr}(L_{\mu\nu} [L^\mu, L^\nu]) + \text{Tr}(R_{\mu\nu} [R^\mu, R^\nu]) \} \\ & + h_2 \text{Tr}(|L_\mu \Phi|^2 + |\Phi R_\mu|^2) + \hat{h}_2 \text{Tr}(|L_\mu \hat{\Phi}|^2 + |\hat{\Phi} R_\mu|^2) + 2h_3 \text{Tr}(L_\mu \Phi R^\mu \Phi^\dagger) + 2\hat{h}_3 \text{Tr}(L_\mu \hat{\Phi} R^\mu \hat{\Phi}^\dagger) \\ & + g_3 [\text{Tr}(L_\mu L_\nu L^\mu L^\nu) + \text{Tr}(R_\mu R_\nu R^\mu R^\nu)] + g_4 [\text{Tr}(L_\mu L^\mu L_\nu L^\nu) + \text{Tr}(R_\mu R^\mu R_\nu R^\nu)], \end{aligned} \quad (9)$$

where $R_{\mu\nu} = \partial_\mu R_\nu - \partial_\nu R_\mu - i[R_\mu, R_\nu]$ and $L_{\mu\nu} = \partial_\mu L_\nu - \partial_\nu L_\mu - i[L_\mu, L_\nu]$. In this Lagrangian, all the terms have $N_q = 8$ at most except the \hat{h}_2 and \hat{h}_3 terms, which are allowed by power-counting rule III.

Next, let us turn to the baryon sector. According to the above discussion, with respect to the chiral and axial invariances, we can write down the effective Lagrangian in term of the basis $N_R^{(\text{RR})}$, $N_L^{(\text{RR})}$, $N_L^{(\text{LL})}$, and $N_R^{(\text{LL})}$ as

$$\begin{aligned} \mathcal{L}_B = & \text{Tr} \left\{ \bar{N}_R^{(\text{RR})} i\gamma_\mu D_{1R}^\mu N_R^{(\text{RR})} + \bar{N}_L^{(\text{RR})} i\gamma_\mu D_{2L}^\mu N_L^{(\text{RR})} + \bar{N}_R^{(\text{LL})} i\gamma_\mu D_{2R}^\mu N_R^{(\text{LL})} + \bar{N}_L^{(\text{LL})} i\gamma_\mu D_{1L}^\mu N_L^{(\text{LL})} \right\} \\ & + 2c' \text{Tr} \left\{ R^\mu \bar{N}_R^{(\text{RR})} \gamma_\mu N_R^{(\text{RR})} + L^\mu \bar{N}_L^{(\text{LL})} \gamma_\mu N_L^{(\text{LL})} \right\} \\ & - g \text{Tr} \left\{ \bar{N}_L^{(\text{RR})} \Phi N_R^{(\text{RR})} + \bar{N}_R^{(\text{RR})} \Phi^\dagger N_L^{(\text{RR})} + \bar{N}_L^{(\text{LL})} \Phi N_R^{(\text{LL})} + \bar{N}_R^{(\text{LL})} \Phi^\dagger N_L^{(\text{LL})} \right\}, \end{aligned} \quad (10)$$

where $D_{iR}^\mu = \partial^\mu - ic_i R^\mu$ and $D_{iL}^\mu = \partial^\mu - ic_i L^\mu$ with c_i being constants. An interesting and important observation from this Lagrangian is that, due to the invariance under axial transformation, only the two-quark component of the scalar fields couples to baryon fields at the lowest order. This is one of the main conclusions of this work.

Without considering the negative parity baryons, one can make the identification

$$\begin{aligned} N_{R,L}^{(\text{RR})} &= \frac{1}{\sqrt{2}} \frac{1 \pm \gamma_5}{2} B, \\ N_{R,L}^{(\text{LL})} &= -\frac{1}{\sqrt{2}} \frac{1 \pm \gamma_5}{2} B, \end{aligned} \quad (11)$$

with B being the baryon octet. Then, the final Lagrangian for baryons to be used in the following is

$$\begin{aligned} \mathcal{L}_B = & \frac{1}{2} \text{Tr} \{ \bar{B} i\gamma_\mu [(D_R^\mu + D_L^\mu) + \gamma_5 (D_R^\mu - D_L^\mu)] B \} \\ & - \frac{g}{2} \text{Tr} \{ \bar{B} [(\Phi + \Phi^\dagger) + \gamma_5 (\Phi - \Phi^\dagger)] B \}, \end{aligned} \quad (12)$$

where $D_R^\mu B = \partial^\mu B - icR^\mu B - ic'BR^\mu$ and $D_L^\mu B = \partial^\mu B - icL^\mu B - ic'BL^\mu$ with c and c' being coupling constants.

B. Physical states

There are two meson multiplets Φ and $\hat{\Phi}$ in the bELSM discussed above. The physical states are the admixture of them. The two-quark nonets can be organized in terms of the scalar and pseudoscalar states as

$$\Phi = S + iP = \begin{pmatrix} \frac{(\sigma_N + a_0^0) + i(\eta_N + \pi^0)}{\sqrt{2}} & a_0^+ + i\pi^+ & K_S^+ + iK^+ \\ a_0^- + i\pi^- & \frac{(\sigma_N - a_0^0) + i(\eta_N - \pi^0)}{\sqrt{2}} & K_S^0 + iK^0 \\ K_S^- + iK^- & \bar{K}_S^0 + i\bar{K}^0 & \sigma_S + i\eta_S \end{pmatrix}. \quad (13)$$

The octet and singlet states can be obtained via

$$\Phi = \frac{1}{\sqrt{2}} \sum_{i=0}^8 \Phi_i \lambda_i = \frac{1}{\sqrt{2}} \left(\sum_{i=0}^8 S_i \lambda_i + i \sum_{i=0}^8 P_i \lambda_i \right), \quad (14)$$

where λ_0 is $\sqrt{\frac{2}{3}} I_{3 \times 3}$ and the others are Gell-Mann matrices. The four-quark configurations can be written in the similar way and will be denoted with an overcared in the following.

Moreover, vector and axial-vector mesons can be obtained through the combination of left- and right-hand currents:

$$(L, R)^\mu = V^\mu \pm A^\mu = \frac{1}{\sqrt{2}} \begin{pmatrix} \frac{\omega_N^\mu + \rho^{\mu 0} \pm f_{1N}^\mu + a_1^{\mu 0}}{\sqrt{2}} & \rho^{\mu+} \pm a_1^{\mu+} & K^{*\mu+} \pm K_1^{\mu+} \\ \rho^{\mu-} \pm a_1^{\mu-} & \frac{\omega_N^\mu - \rho^{\mu 0} \pm f_{1N}^\mu - a_1^{\mu 0}}{\sqrt{2}} & K^{*\mu 0} \pm K_1^{\mu 0} \\ K^{*\mu-} \pm K_1^{\mu-} & \bar{K}^{*\mu 0} \pm \bar{K}_1^{\mu 0} & \omega_S^\mu \pm f_{1S}^\mu \end{pmatrix}. \quad (15)$$

Finally, the baryon octet takes the form

$$B \equiv \begin{pmatrix} \frac{\Lambda}{\sqrt{6}} + \frac{\Sigma^0}{\sqrt{2}} & \Sigma^+ & p \\ \Sigma^- & \frac{\Lambda}{\sqrt{6}} - \frac{\Sigma^0}{\sqrt{2}} & n \\ \Xi^- & \Xi^0 & -\frac{2\Lambda}{\sqrt{6}} \end{pmatrix}. \quad (16)$$

$$\begin{bmatrix} \Phi_{i,j} \\ \hat{\Phi}_{i,j} \end{bmatrix} = R \begin{bmatrix} \Phi'_{i,j} \\ \hat{\Phi}'_{i,j} \end{bmatrix} = \begin{bmatrix} \cos \theta_{i,j} & -\sin \theta_{i,j} \\ \sin \theta_{i,j} & \cos \theta_{i,j} \end{bmatrix} \begin{bmatrix} \Phi'_{i,j} \\ \hat{\Phi}'_{i,j} \end{bmatrix}, \quad (18)$$

At low energies, the chiral symmetry of QCD breaks to $U(3)_V$ spontaneously, so it is more reasonable to let the scalar components which lie on the diagonal position of the Φ matrix to have nonzero vacuum expectation values

$$\langle S_a^b \rangle = \alpha_a \delta_a^b, \quad \langle \hat{S}_a^b \rangle = \beta_a \delta_a^b, \quad (17)$$

where S_a^b and \hat{S}_a^b stand for the two-quark and four-quark scalar components, respectively. Certainly, $\alpha_1 = \alpha_2 = \alpha_3 = \alpha$ and $\beta_1 = \beta_2 = \beta_3 = \beta$ if $U(3)_V$ symmetry is exact. Then the fluctuations of the two- and four-quark fields are defined as $\tilde{S}_a^b = S_a^b - \alpha \delta_a^b$ and $\tilde{\hat{S}}_a^b = \hat{S}_a^b - \beta \delta_a^b$, respectively.

The existence of c_3 and e_3 terms in V_0 leads to the mixing of two-quark and four-quark states. The mixing angles can be obtained by solving two-point vertex functions, and the mixing matrix can be defined as

$$\Psi = \begin{pmatrix} p \\ n \end{pmatrix},$$

where the superscript prime denotes the physical states. Currently, it leads to four mixing sets of (pseudo)scalar sectors (octets and singlets).

The four-quark configurations follow the same terminology. Then, the minimum potential conditions should also be considered in order to pin down vacuum expectation values of isoscalar-scalar states, α and β :

$$\begin{aligned} \left\langle \frac{\partial V_0}{\partial S_{a,a}} \right\rangle &= 2\alpha(-c_2 + 2c_4\alpha^2 + 4e_3\beta) = 0, \\ \left\langle \frac{\partial V_0}{\partial \hat{S}_{a,a}} \right\rangle &= 2(d_2\beta + 2e_3\alpha^2) = 0. \end{aligned} \quad (19)$$

In this work, we will not consider strange hadrons or mesons heavier than 1 GeV. And, since EOS of nuclear matter is obtained via RMF approximation, the axial-vector and pseudoscalar mesons will also be dropped out. Then the baryon field B can be rewritten as

and the relevant mesons should be scalar and vector mesons including $f_0(500)$ (denoted as σ), $f_0(980)$, $a_0(980)$, ω , and ρ .

C. Physical parameters

The physical parameters can be defined in terms of the parameters in the above discussed Lagrangian and the corresponding mixing angles. By diagonalizing of two-point effective potentials, one can obtain mass terms for scalar singlets and scalar octets, respectively, as

$$\begin{aligned} m_{s,0,\pm} &= -c_2 + 6\alpha^2 c_4 + d_2 + 4\beta e_3 \pm \sqrt{(-c_2 + 6\alpha^2 c_4 + d_2 + 4\beta e_3)^2 + 4(c_2 d_2 - 6\alpha^2 c_4 d_2 + 4e_3(4\alpha^2 e_3 - \beta d_2))}, \\ m_{s,8,\pm} &= -c_2 + 6\alpha^2 c_4 + d_2 - 2\beta e_3 \pm \sqrt{(c_2 - 6\alpha^2 c_4 - d_2 + 2\beta e_3)^2 + 4(c_2 d_2 - 6\alpha^2 c_4 d_2 + 2e_3(2\alpha^2 e_3 + \beta d_2))}. \end{aligned} \quad (20)$$

It is obvious that one stands for the light states and the other one stands for heavier ones, and the mixing angle in Eq. (18) can be also obtained as

$$\begin{aligned} \theta_{s,0} &= -\frac{1}{2} \arctan\left(\frac{8\alpha e_3}{c_2 - 6\alpha^2 c_4 - 4\beta e_3 + d_2}\right), \\ \theta_{s,8} &= -\frac{1}{2} \arctan\left(\frac{4\alpha e_3}{c_2 - 6\alpha^2 c_4 + 2\beta e_3 + d_2}\right). \end{aligned} \quad (21)$$

With the above arguments, the Lagrangian contributing to the mean field approach can be written as

$$\mathcal{L}_{\text{RMF}} = \bar{\Psi}(i\not{\partial} - m_N)\Psi + \mathcal{L}_\sigma + \mathcal{L}_\omega + \mathcal{L}_\rho + \mathcal{L}_{a_0} + \mathcal{L}_{f_0} + \mathcal{L}_I, \quad (22)$$

where $m_N = g\alpha$. The Lagrangian for the meson part can be organized as

$$\begin{aligned} \mathcal{L}_\sigma &= \frac{1}{2}(\partial_\mu \sigma \partial^\mu \sigma - m_\sigma^2 \sigma^2), \\ \mathcal{L}_\omega &= -\frac{1}{4}\omega_{\mu\nu}\omega^{\mu\nu} + \frac{1}{2}m_\omega^2 \omega_\mu \omega^\mu, \\ \mathcal{L}_\rho &= -\frac{1}{4}\vec{\rho}_{\mu\nu} \cdot \vec{\rho}^{\mu\nu} + \frac{1}{2}m_\rho^2 \vec{\rho}_\mu \cdot \vec{\rho}^\mu, \\ \mathcal{L}_{a_0} &= \frac{1}{2}(\partial_\mu \vec{a}_0 \cdot \partial^\mu \vec{a}_0 - m_{a_0}^2 \vec{a}_0^2), \\ \mathcal{L}_{f_0} &= \frac{1}{2}(\partial_\mu f_0 \partial^\mu f_0 - m_{f_0}^2 f_0^2), \end{aligned} \quad (23)$$

where $a_0 = a_0^i \tau^i$, $\rho_\mu = \rho_\mu^i \tau^i$ with τ^i being the Pauli matrices, and

$$\begin{aligned} m_\rho &= m_\omega \\ &= \sqrt{2h_2\alpha^2 + 2\hat{h}_2\beta^2 + 2h_3\alpha^2 + 2\hat{h}_3\beta^2}. \end{aligned} \quad (24)$$

The interaction terms can be written as

$$\begin{aligned} \mathcal{L}_I &= \bar{\Psi}(g_{a_0 NN} a_0 + g_{f_0 NN} f_0 + g_{\sigma NN} \sigma \\ &\quad + g_{\rho NN} \gamma_\mu \rho^\mu + g_{\omega NN} \gamma_\mu \omega^\mu)\Psi + \mathcal{L}_3 + \mathcal{L}_4, \end{aligned} \quad (25)$$

where $g_{a_0 NN} = -\frac{1}{\sqrt{2}}g \cos \tilde{\theta}_{s,8}$, $g_{f_0 NN} = -\frac{g}{\sqrt{6}} \cos \tilde{\theta}_{s,8}$, $g_{\sigma NN} = -\frac{g}{\sqrt{3}} \cos \tilde{\theta}_{s,0}$, and $g_{\rho NN} = g_{\omega NN} = \frac{c}{2}$. $\tilde{\theta}$ can be θ or $\frac{\pi}{2} + \theta$ defined in Eq. (21) corresponding to the choice of light set between $\Phi'_{i,j}$ and $\hat{\Phi}'_{i,j}$. $\mathcal{L}_{3(4)}$ refers to three-(four-) meson coupling terms which are listed in the Appendix.

Note that with RMF approximation only zero components in isospin space and nonderivative terms in Lorentz space survive for meson fields. Therefore, g_1 and g_2 make no contribution and the effects of g_4 , h_3 , and \hat{h}_3 can be absorbed by g_3 , h_2 , and \hat{h}_2 , respectively.

III. PHENOMENOLOGICAL ANALYSIS AND NUMERICAL RESULTS

A. Parameter values

The parameters interrelated in this work are α , β , c_2 , c_4 , d_2 , e_3 , h_2 , \hat{h}_2 , g_3 , and c . By using Eq. (19), two parameters, e.g., d_2 and c_2 , can be reduced. The other parameters are determined by pinning the empirical values of meson spectrums and nuclear matter properties. Our results are listed in Table I. In the following, this set of parameters is denoted as ‘‘opt.’’

The light isosinglet scalar meson σ takes the choice of $\tilde{\theta} = \theta$, and the light mesons a_0 and f_0 in the original octet take the choice of $\tilde{\theta} = \theta + \frac{\pi}{2}$, where $\theta_{s,0} = 41.0^\circ$ and $\theta_{s,8} = 40.7^\circ$, which indicates the two-quark component in the singlet is 56.9% and that in the octet is 42.5%. This

TABLE I. Values of the parameters interrelated in this work. α and β are in units of MeV, and e_3 is in units of GeV.

α	β	e_3	c_4	h_2	\hat{h}_2	g_3	c
32.3	9.55	-3.58	154	370	-915	630	25.8

TABLE II. The spectrums of hadrons in units of MeV. The empirical values are chosen as the real parts of the corresponding resonance T-matrix poles from Ref. [47]. The excited state f'_0 is chosen to be $f_0(1370)$ with a'_0 being $a_0(1450)$ and σ' being $f_0(1500)$. Since $U(3)_V$ is exact in the current work, the empirical values for ρ and ω $f_0(1370)$ and $a_0(1450)$ are combined together. The nucleon mass is fixed as 938 MeV for simplicity.

	m_N	m_σ	$m_{f_0(a_0)}$	$m_{f'_0(a'_0)}$	$m_{\sigma'}$	$m_{\rho(\omega)}$
Empirical	938–940	400–800	960–1010	1250–1500	1430–1530	761–783
opt	938	701	965	1359	1526	779

TABLE III. Nuclear matter properties at saturation density n_0 . e_0 is the binding energy of nucleon, $E_{\text{sym}}(n) = \frac{1}{2} \frac{\partial^2 E(n,a)}{\partial a^2} \Big|_{a=0}$ is the symmetry energy, $K_0 = 9n_0^2 \frac{\partial^2 E(n,0)}{\partial n^2} \Big|_{n=n_0}$ is the incompressibility coefficient, $J_0 = 27n_0^3 \frac{\partial^3 E(n,0)}{\partial n^3} \Big|_{n=n_0}$ is the skewness coefficient, and $L_0 = 3n_0 \frac{\partial E_{\text{sym}}(n_0)}{\partial n} \Big|_{n=n_0}$ is the symmetry energy density slope.

	$n_0(\text{fm}^{-3})$	e_0 (MeV)	$E_{\text{sym}}(n_0)$ (MeV)	J_0 (MeV)	L_0 (MeV)	K_0 (MeV)
Empirical	0.155 ± 0.050 [48]	-15.0 ± 1.0 [48]	30.9 ± 1.9 [49]	-700 ± 500 [50]	52.5 ± 17.5 [49]	230 ± 30 [51]
Opt	0.155	-16.0	31.9	-449	62.7	225

leads to $g_{\sigma NN} = -13.0$, $g_{a_0 NN} = 13.8$, $g_{f_0 NN} = 7.98$, and $g_{\rho(\omega) NN} = 12.7$.

The three-(four-)meson couplings $\mathcal{L}_{3(4)}$ after RMF simplification are organized as

$$\begin{aligned} \mathcal{L}_3 = & -m_N(-13.2a_0^2 f_0 + 4.41f_0^3 + 1.84f_0\rho^2 + 9.72a_0^2\sigma + 9.72f_0^2\sigma - 4.06\rho^2\sigma + 1.96\sigma^3 \\ & + 6.36a_0\rho\omega + 1.84f_0\omega^2 - 4.06\omega^2\sigma) \end{aligned} \quad (26)$$

and

$$\begin{aligned} \mathcal{L}_4 = & -13.9a_0^4 - 27.8a_0^2 f_0^2 - 13.9f_0^4 + 116a_0^2\rho^2 - 38.6f_0^2\rho^2 + 158\rho^4 + 90.9a_0^2 f_0\sigma - 30.3f_0^3\sigma \\ & + 98.7f_0\rho^2\sigma - 74.4a_0^2\sigma^2 - 74.4f_0^2\sigma^2 - 61.2\rho^2\sigma^2 - 16.6\sigma^4 - 267a_0 f_0\rho\omega + 342a_0\rho\sigma\omega \\ & - 116a_0^2\omega^2 - 38.6f_0^2\omega^2 + 946\rho^2\omega^2 + 98.7f_0\sigma\omega^2 - 61.2\sigma^2\omega^2 + 158\omega^4, \end{aligned} \quad (27)$$

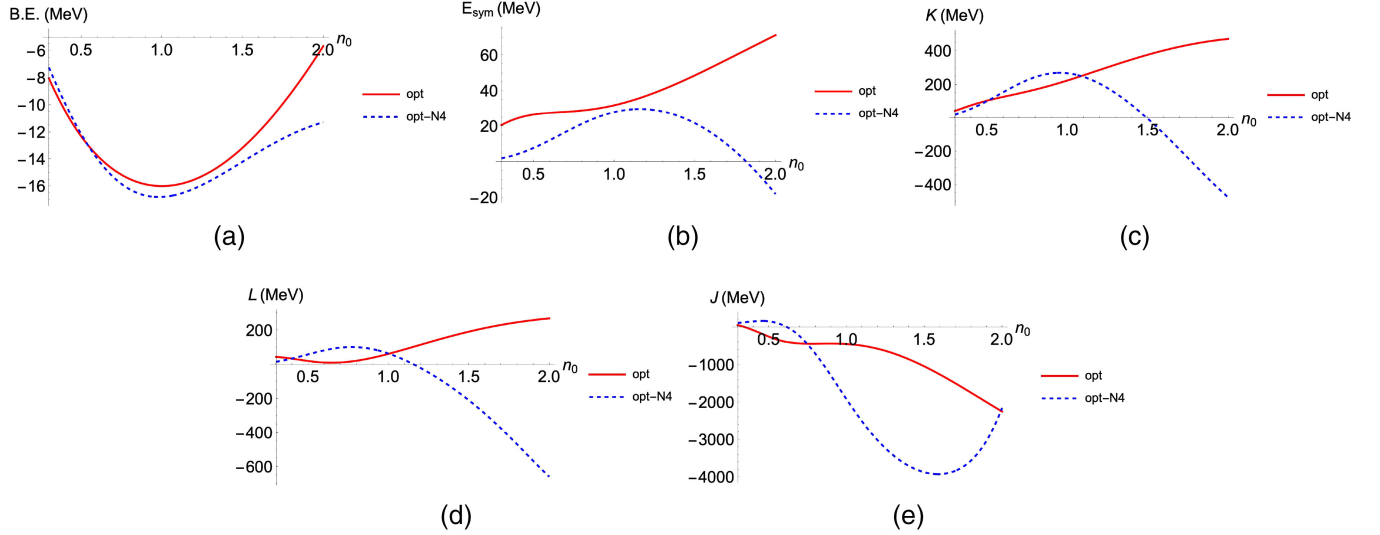
where, to clearly show the magnitudes of the contributions, we explicitly write down the values of the coupling constants. The above parameter space leads to the spectrums of mesons and nuclear matter quantities listed in Tables II and III, respectively.

It can be seen that the choice of parameter space opt leads to reasonable physical results. In the numerical calculation is found $\alpha \simeq 30$ MeV, which makes $|g_{\sigma NN}| \sim 10$, in order to obtain the physical quantities of NM. The $g_{\sigma NN}$ is consistent with Refs. [17,28,41,42,52], where the couplings between sigma and nucleon are parametrized as one-boson-exchange (OBE) form. It provides evidence that this model is suited for the description of NM properties and also makes a suggestion that m_σ may be around 700 MeV in the nuclear medium.

B. Parameter dependence of nuclear matter properties

The couplings between scalar mesons and nucleons contribute to attractive potential, while those between

vector mesons and nucleons contribute to repulsive potential, and the competition between them leads to the saturation of NM and the value of e_0 . After obtaining the reasonable e_0 in current bELSM, the K_0 and $E_{\text{sym}}(n_0)$ are found to be too large compared to experimental data. Then, the four-vector meson self-interaction term g_3 is found to be crucial to suppress these higher-order density-dependent quantities. But, when pinning down all these quantities, the choice of g_3 makes the E_{sym} and K to be negative, which may lead to a too soft neutron star structure in the current scheme. With this, the importance of the four-quark configuration \hat{h}_2 term comes in and compensates the effects brought by g_3 terms at high-density regions while keeping higher-order quantities at n_0 reasonable. In addition, the \hat{h}_2 terms yield $|g_{\omega NN}| \simeq 13$, which is also consistent with the models in Refs. [17,28,41,42,52]. These effects can be seen in Fig. 1, where opt and opt-N4 which refers to the parameter set without \hat{h}_2 terms are compared. In opt-N4, the parameters are chosen as $\alpha = 35.8$ MeV,


 FIG. 1. (a)–(e) Comparison between models with (opt) and without \hat{h}_2 (opt-N4) terms.

$\beta = 8.03$ MeV, $c_4 = 146$, $e_3 = -2640$ MeV, $h_2 = 232$, $c = 14.6$, and $g_3 = 123$ in order to pin down the NM properties, and this choice yields $g_{\omega NN} = 7.28$ with $m_\sigma = 910$ MeV.

We next investigate the effects of each parameter on the NM properties by changing 1% of the opt values. The effects on the spectrum are shown in Tables IV and V, and those on NM properties are illustrated in Figs. 2–6.

From Fig. 2, it can be seen that the binding energy is sensitive to α , β , c_4 , e_3 , and c , since these parameters determine the spectra and couplings between nucleons and mesons. As expected, multimeson couplings, the g_3 , h_2 , and \hat{h}_2 terms, affect less because they represent higher-order density dependence. In general, the binding energy is consistent with TM1 [41] and FSU- $\delta 6.7$ [28]. So, its

behavior is similar to the previous conclusion which is determined by the competition between attractive and repulsive potentials.

The parameter dependence of the symmetry energy E_{sym} is shown in Fig. 3. A generic property which can be found is the existence of a plateaulike structure which is due to the possible multimeson couplings allowed by chiral symmetry and power-counting rules set up above. Actually, this structure has also been found in FSU- $\delta 6.7$ [28] to describe the neutron skin thickness of ^{208}Pb and tidal deformability of neutron stars. Explicitly, the ^{208}Pb measurement suggests that $L(2/3n_0)$ (E_{sym} slope) should be larger than 49 MeV, and the neutron star tidal deformation (TD) $\Lambda_{1.4}$ is estimated as 642–955 [53], if E_{sym} is stiff at intermediate densities. Such a calculated value of

 TABLE IV. The effects on spectra and two-quark configuration by parameter variation. opt-a \pm refers to the parameter set with $\tilde{\alpha} = (1 \pm 0.01)\alpha$ with α being the value in opt. The same convention is used for other parameters with b for β , c4 for c_4 , and e for e_3 .

	opt-a+	opt-a–	opt-b+	opt-b–	opt-c4+	opt-c4–	opt-e3+	opt-e3–
m_σ (MeV)	715	687	696	706	706	696	699	703
m_{a_0} (MeV)	974	956	969	960	973	956	961	968
m_ω (MeV)	789	770	777	782	779	779	779	779
σ two-quark (%)	56.5	57.2	57.9	55.8	57.6	56.2	56.2	57.6
a_0 two-quark (%)	42.4	42.6	42.9	42.1	42.8	42.2	42.2	42.8

 TABLE V. The effects on vector spectra. The notations are the same as Table IV: h for h_2 , H for \hat{h}_2 , g for g_3 , and c for c .

	opt-c+	opt-c–	opt-h2+	opt-h2–	opt-g3+	opt-g3–	opt-H2+	opt-H2–
m_ω (MeV)	779	779	784	774	780	780	778	781

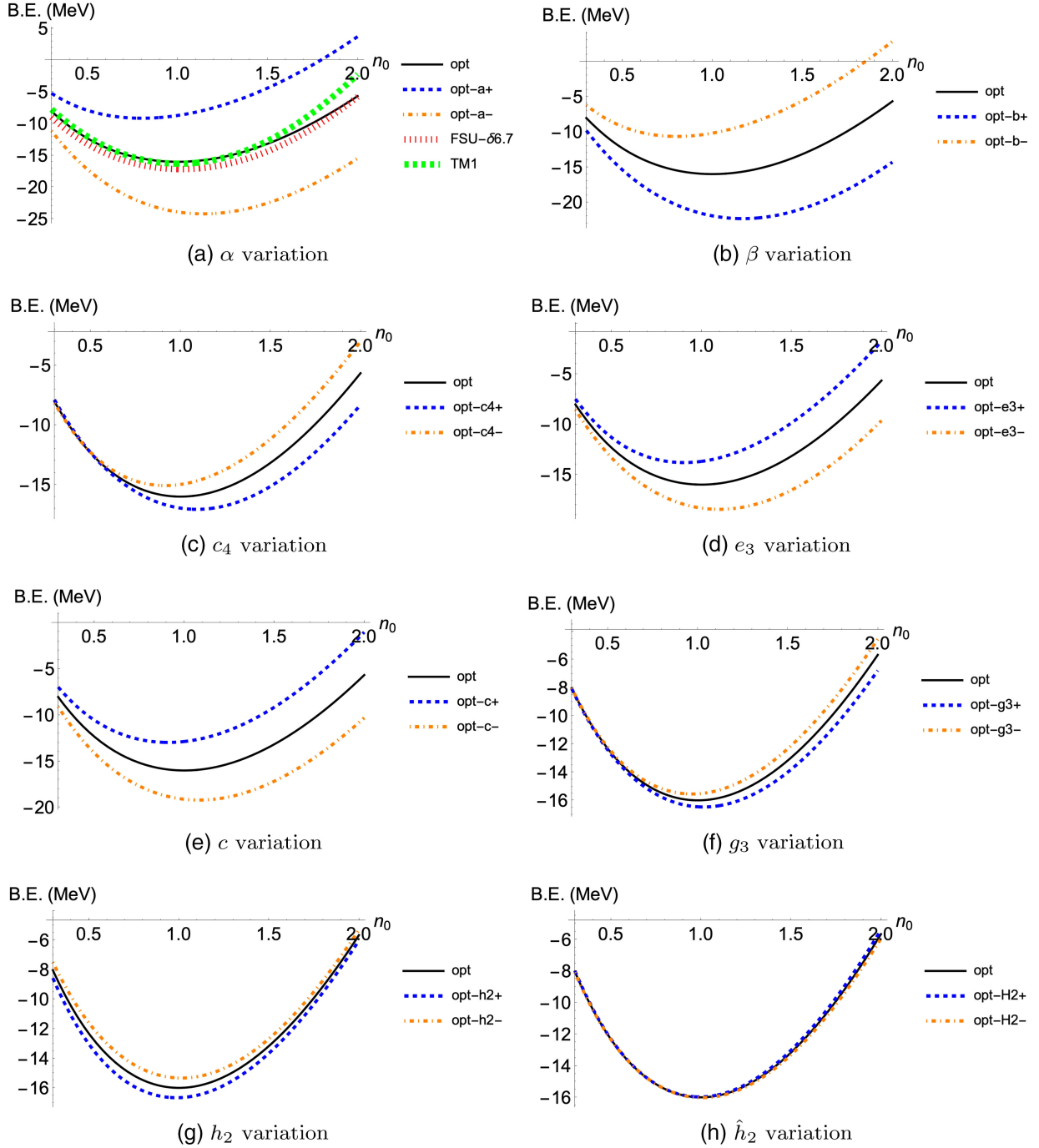


FIG. 2. Parameter effects on the binding energy. TM1 is the result from Ref. [41], where ρ , ω , and σ mesons are considered with $n_0 = 0.145 \text{ fm}^{-3}$. FSU- $\delta 6.7$ is the result from Ref. [28], where δ [here, $a_0(980)$] meson is added with $n_0 = 0.148 \text{ fm}^{-3}$.

$\Lambda_{1.4}$ is larger than the one extracted from GW170817 $\Lambda_{1.4} \leq 580$ [54]. In order to yield the neutron star TD consistent with both GW170817 and neutron skin thickness of ^{208}Pb , the symmetry energy should be stiff at subsaturation densities but soft at intermediate regions, leading to a plateaulike structure in symmetry energy. The difference is that the plateaulike structure in this work appears at a lower-density region than that in FSU- $\delta 6.7$.

The reason is that the current bELSM is built with exact $U(3)_V$ symmetry, which sets $g_{\rho NN} = g_{\omega NN}$ and also constrains other vector meson couplings. With these constraints, the E_{sym} will first increase to a large value when the binding energy is tuned to a reasonable value by adjusting $g_{\omega NN}$, but the growth rate of E_{sym} must be suppressed around n_0 to meet the requirement $E_{\text{sym}} \approx 32 \text{ MeV}$.

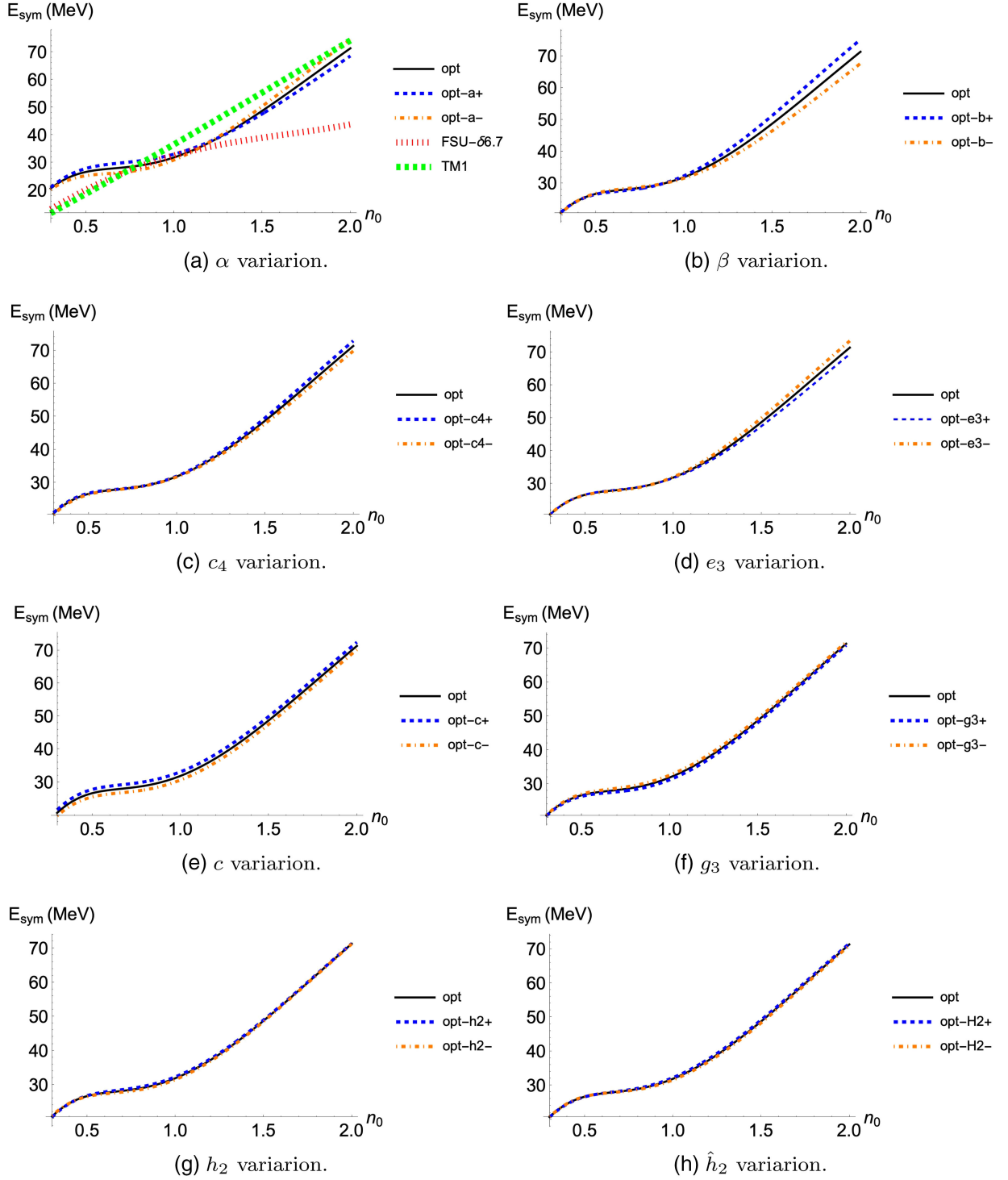


FIG. 3. Parameter effects on symmetry energy E_{sym} . (a) α variation. (b) β variation. (c) c_4 variation. (d) e_3 variation. (e) c variation. (f) g_3 variation. (g) h_2 variation. (h) \hat{h}_2 variation.

This reasoning based on the symmetry argument can also be seen in the analysis of the slope of the symmetry energy L . From Fig. 4, one can see that there is quantitative difference between opt and FSU- $\delta 6.7$ due to the exact $U(3)_V$ symmetry applied here, but the qualitative behavior is similar. The valley structure of the slope

around $0.6n_0$ yields the plateaulike structure of E_{sym} below n_0 and gives a realistic E_{sym} . In addition, it is found that the slope is affected mainly by the quark condensates. It is reasonable to expect that the behavior of L can be revised by breaking the $U(3)_V$ symmetry into $SU(3)_V \times U(1)_V$.

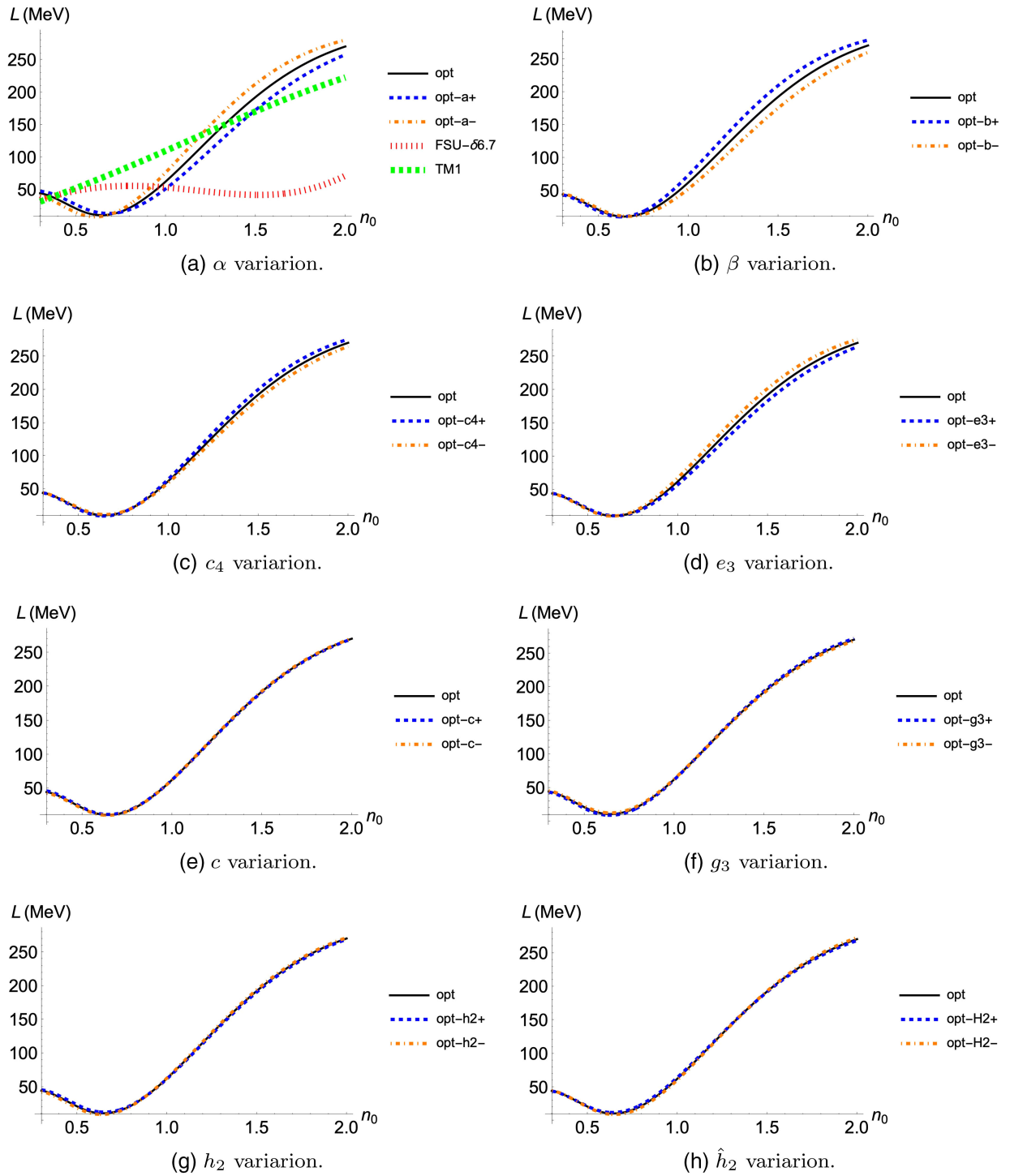


FIG. 4. Parameter effects on the slope of the symmetry energy L . (a) α variation. (b) β variation. (c) c_4 variation. (d) e_3 variation. (e) c variation. (f) g_3 variation. (g) h_2 variation. (h) \hat{h}_2 variation.

It is found in Fig. 5 that the variations of α , β , and c increase or decrease K at all regions below $2n_0$, while those multimeson coupling contributions are opposite between regions below and above n_0 , especially those triple- and quadruple-scalar-meson couplings. The behavior of K can affect the speed of sound v_s NM. Explicitly, a large K

always leads to a large v_s by definition. v_s is at the center of the stage in the studies on strong interaction in dense systems, since its unique behavior always indicates interesting phenomena [55–59]. The analysis here may provide some hints about introducing multimeson couplings in a more logical way.

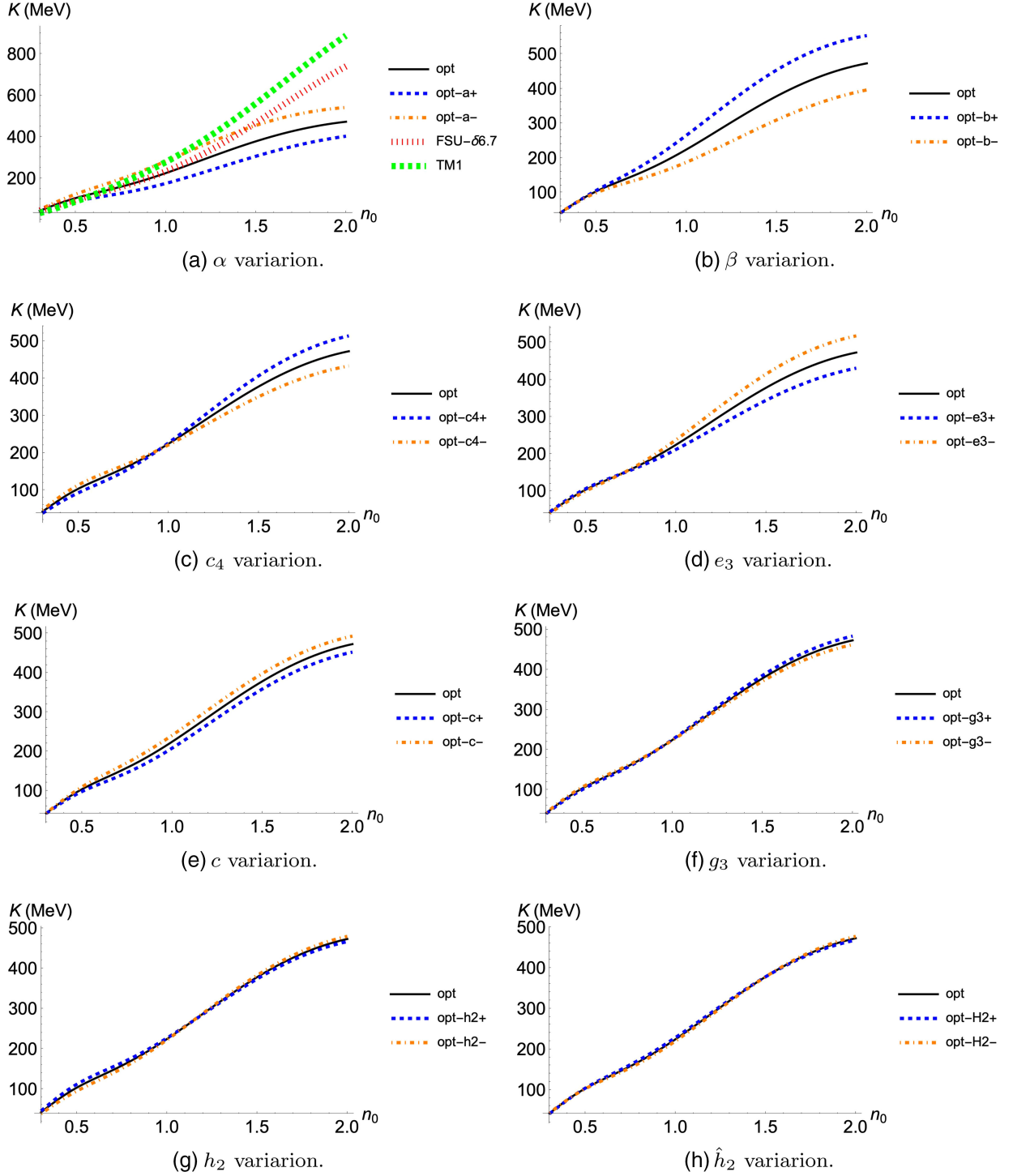


FIG. 5. Parameter effects on incompressibility coefficient K . (a) α variation. (b) β variation. (c) c_4 variation. (d) e_3 variation. (e) c variation. (f) g_3 variation. (g) h_2 variation. (h) \hat{h}_2 variation.

Different from other properties discussed above, the constraint on the skewness coefficient J_0 is not well understood, and it varies between -1200 and 400 MeV based on different targets or analysis methods [50,60,61]. An interesting point is that a plateaulike structure is found in every model from Fig. 6. The parameter variation effects

are similar to that in the incompressibility K ; that is, the multimeson coupling contributions are opposite between high-density regions and low-density regions.

The above analysis shows that the stiffness of the EOS obtained with the parameter choice *opt* is different from other approaches, for example, FSU- $\delta 6.7$, due to the $U(3)_V$

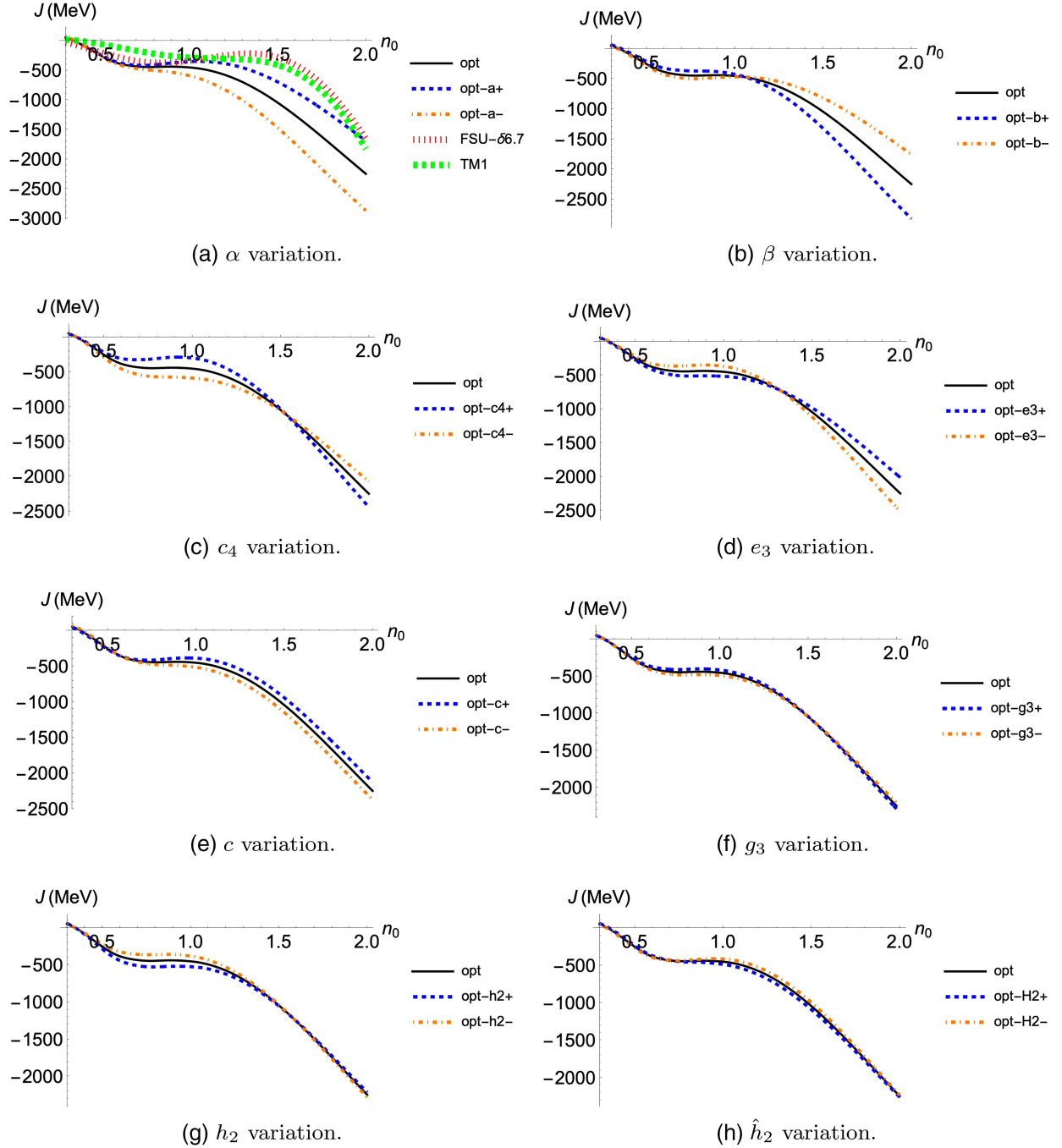


FIG. 6. Parameter effects on skewness coefficient J . (a) α variation. (b) β variation. (c) c_4 variation. (d) e_3 variation. (e) c variation. (f) g_3 variation. (g) h_2 variation. (h) \hat{h}_2 variation.

symmetry applied. Using the parameter choice opt, we found that the maximum mass of neutron star is $1.98M_\odot$, and the radius of the neutron star with mass $1.4M_\odot$ neutron star is 14.5 km with the tidal deformability $\Lambda_{1.4} = 1440$. Obviously, the neutron star predicted above is less compact than expected to describe the GW170817 event and the tidal deformability is beyond the constraint. The possible

reasons are the following: (i) The $U(3)_V$ symmetry should break into $SU(3)_V \times U(1)_V$, especially in a dense environment [62]; (ii) the explicit chiral symmetry-breaking terms are important because too strong multimeson couplings are introduced to obtain reasonable spectrums without quark mass terms, and it may cause too much noise at high-density regions.

IV. DISCUSSION AND PERSPECTIVE

In this work, a bELSM is built to study the properties of nuclear matter with special interest in the effects of quark configurations of scalar mesons and vector resonances. The model is built with three flavors such that the splitting of scalar meson octet and singlet can be analyzed and the a_0 and f_0 mesons can be included with σ meson in a unified framework.

By pinning down the spectra of mesons and NM properties at saturation density with RMF approximation, the parameters are determined. It is found that the NM properties are sensitive to the two-quark condensate α , which determines the couplings between scalar mesons and nucleons, and $|g_{\sigma NN}|$ should be around $\simeq 10$. This result is consistent with previous works where σ is parametrized as OBE form.

We find that there is a plateaulike structure in the E_{sym} curve because of the valley structure in its slope L . This behavior has already been addressed in Ref. [28], where $a_0(980)$, also known as δ , is introduced to produce the plateaulike structure to describe neutron skin thickness and tidal deformation of neutron star (NS) constraints at the same time. But the plateaulike structure appears too early in current bELSM due to $U(3)_V$ symmetry applied, which sets $g_{\rho NN} = g_{\omega NN}$ making E_{sym} grow too rapidly below n_0 . This implies that $U(3)_V$ symmetry is necessarily broken into $SU(3)_V \times U(1)_V$ in a dense environment. And, because of the early plateaulike structure, the star properties are slightly beyond the constraints of GW170817.

Besides the breaking of the $U(3)_V$ symmetry, another factor that may remedy the drawback of the present model

is the explicit chiral symmetry-breaking effect which is not considered in the present work. This is because the quark masses may apparently reduce the strength of multimeson couplings producing the meson spectra in current bELSM. This effect will be studied in a forthcoming work.

With more and more NS signals detected, the more stringent multisource constraints of nucleon interactions in the medium will become available. Therefore, a systematic investigation of the hadron spectrum, NM properties, and neutron star properties will bring insights into strong interactions and the nature of hadrons, such as the structure of light scalar mesons. The present model will be a good starting point to further explore in a wider density range of NM.

In the future, the bELSM will be extended to a more realistic one with a better symmetry pattern to describe the neutron stars with RMF approximation, and the strange freedoms will also be considered naturally. In addition, it is also interesting to introduce the quantum effects of hadrons using the bELSM with the Hartree-Fock method, so that the contributions of pseudoscalar and axial-vector mesons can be included. All these will be clarified in forthcoming works.

ACKNOWLEDGMENTS

The work of Y.-L. M. is supported in part by the National Key R&D Program of China under Grant No. 2021YFC2202900 and the National Science Foundation of China (NSFC) under Grants No. 11875147 and No. 12147103.

APPENDIX: THE TRIPLE-MESON AND QUADRUPLE-MESON COUPLINGS

In this appendix, we explicitly list the triple-meson couplings and quadruple-meson couplings which contribute to the present calculation after the RMF.

The triple-meson couplings that survive under RMF are the following:

$$\begin{aligned}
\mathcal{L}_3 = & -\frac{1}{6} \left(12\sqrt{3}c_4f_0^2\alpha\sigma\cos\theta_0 - 4\sqrt{3}h_2a\rho^2\sigma\cos\theta_0 + 6\sqrt{3}c_4\alpha\sigma^3\cos\theta_0 - 4\sqrt{3}h_2\alpha\sigma\omega^2\cos\theta_0 \right. \\
& + 2\sqrt{3}c_4\alpha\sigma^3\cos(3\theta_0) - 6\sqrt{3}c_4f_0^2\alpha\sigma\cos(\theta_0 - 2\theta_8) - \sqrt{6}e_3f_0^3\cos\theta_8 \\
& + \sqrt{6}e_3f_0^3\cos(3\theta_8) - 6\sqrt{3}c_4f_0^2\alpha\sigma\cos(\theta_0 + 2\theta_8) - 2\sqrt{3}e_3f_0^2\sigma\sin\theta_0 \\
& - 4\sqrt{3}\hat{h}_2\beta\rho^2\sigma\sin\theta_0 + 2\sqrt{3}e_3\sigma^3\sin\theta_0 - 4\sqrt{3}\hat{h}_2\beta\sigma\omega^2\sin\theta_0 + 2\sqrt{3}e_3\sigma^3\sin(3\theta_0) \\
& - \sqrt{3}e_3f_0^2\sigma\sin(\theta_0 - 2\theta_8) + 3\sqrt{6}c_4f_0^3\alpha\sin(\theta_8) + 2\sqrt{6}h_2f_0a\rho^2\sin\theta_8 + 2\sqrt{6}\hat{h}_2\beta f_0\rho^2\sin\theta_8 \\
& + 12\sqrt{2}h_2a_0\rho\omega\sin\theta_8 + 12\sqrt{2}\hat{h}_2\beta a_0\rho\omega\sin\theta_8 + 2\sqrt{6}\hat{h}_2\alpha f_0\omega^2\sin\theta_8 + 2\sqrt{6}\hat{h}_2\beta f_0\omega^2\sin\theta_8 \\
& + 8\sqrt{3}e_3a_0^2\sigma\cos\theta_0\cos\theta_8\sin\theta_8 + 24\sqrt{3}c_4\alpha\sigma a_0^2\cos\theta_0\sin^2\theta_8 + 12\sqrt{6}e_3f_0a_0^2\cos\theta_8\sin\theta_8^2 \\
& - 4\sqrt{3}e_3\sigma a_0^2\sin\theta_0\sin^2\theta_8 - 12\sqrt{6}c_4\alpha f_0a_0^2\sin^3\theta_8 - \sqrt{6}c_4f_0^3\alpha\sin(3\theta_8) \\
& \left. + 3\sqrt{3}e_3f_0^2\sigma\sin(\theta_0 + 2\theta_8) \right). \tag{A1}
\end{aligned}$$

The quadruple-meson couplings contributing to the present calculation are summarized as

$$\begin{aligned}
\mathcal{L}_4 = & -\frac{1}{48}(9c_4f_0^4 - 4h_2f_0^2\rho^2 - 4\hat{h}_2f_0^2\rho^2 - 12g_3\rho^4 + 24c_4f_0^2\sigma^2 - 8h_2\rho^2\sigma^2 - 8\hat{h}_2\rho^2\sigma^2 + 6c_4\sigma^4 \\
& - 4h_2f_0^2\omega^2 - 4\hat{h}_2f_0^2\omega^2 - 72g_3\rho^2\omega^2 - 8h_2\sigma^2\omega^2 - 8\hat{h}_2\sigma^2\omega^2 - 12g_3\omega^4 \\
& + 24c_4f_0^2\sigma^2\cos(2\theta_0) - 8h_2\rho^2\sigma^2\cos(2\theta_0) + 8\hat{h}_2\rho^2\sigma^2\cos(2\theta_0) + 8c_4\sigma^4\cos(2\theta_0) \\
& - 8h_2\sigma^2\omega^2\cos(2\theta_0) + 8\hat{h}_2\sigma^2\omega^2\cos(2\theta_0) + 2c_4\sigma^4\cos(4\theta_0) + 8\sqrt{2}\hat{h}_2f_0\rho^2\sigma\cos(\theta_0 - \theta_8) \\
& + 8\sqrt{2}\hat{h}_2f_0\sigma\omega^2\cos(\theta_0 - \theta_8) - 12c_4f_0^2\sigma^2\cos[2(\theta_0 - \theta_8)] - 12c_4f_0^4\cos[2\theta_8] \\
& + 4h_2f_0^2\rho^2\cos(2\theta_8) + 4\hat{h}_2f_0^2\rho^2\cos\theta_8 - 24c_4f_0^2\sigma^2\cos\theta_8 + 4h_2f_0^2\omega^2\cos\theta_8 \\
& + 4\hat{h}_2f_0^2\omega^2\cos\theta_8 + 3c_4f_0^4\cos\theta_8 - 8\sqrt{2}\hat{h}_2f_0\rho^2\sigma\cos(\theta_0 + \theta_8) - 8\sqrt{2}\hat{h}_2f_0\sigma\omega^2\cos(\theta_0 + \theta_8) \\
& - 12c_4f_0^2\sigma^2\cos[2(\theta_0 + \theta_8)] + 4\sqrt{2}c_4f_0^3\sigma\sin(\theta_0 - 3\theta_8) - 12\sqrt{2}c_4f_0^3\sigma\sin(\theta_0 - \theta_8) \\
& - 8\sqrt{2}h_2f_0\rho^2\sigma\sin[\theta_0 - \theta_8] - 8\sqrt{2}h_2f_0\sigma\omega^2\sin(\theta_0 - \theta_8) + 32\sqrt{6}h_2a_0\rho\sigma\omega\cos\theta_0\sin\theta_8 \\
& + 32\sqrt{6}\hat{h}_2a_0\rho\sigma\omega\sin\theta_0\sin\theta_8 - 24h_2a_0^2\rho^2\sin^2\theta_8 - 24\hat{h}_2a_0^2\rho^2\sin^2\theta_8 \\
& - 32\sqrt{3}h_2a_0f_0\rho\omega\sin^2\theta_8 - 32\sqrt{3}\hat{h}_2a_0f_0\rho\omega\sin^2\theta_8 - 24h_2a_0^2\omega^2\sin^2\theta_8 - 24\hat{h}_2a_0^2\omega^2\sin^2\theta_8 \\
& + 96c_4a_0^2\sigma^2\cos^2\theta_0\sin^2\theta_8 - 96\sqrt{2}c_4a_0^2f_0\sigma\cos\theta_0\sin\theta_8^3 + 24c_4a_0^4\sin\theta_8^4 + 48c_4a_0^2f^2\sin\theta_8^4 \\
& + 12\sqrt{2}c_4f_0^3\sigma\sin(\theta_0 + \theta_8) + 8\sqrt{2}h_2f_0\rho^2\sigma\sin(\theta_0 + \theta_8) \\
& + 8\sqrt{2}h_2f_0\sigma\omega^2\sin(\theta_0 + \theta_8) - 4\sqrt{2}c_4f_0^3\sigma\sin(\theta_0 + 3\theta_8)), \tag{A2}
\end{aligned}$$

where the mixing angles have already been chosen based on the numerical results in Sec. III.

-
- [1] B. D. Serot and J. D. Walecka, *Adv. Nucl. Phys.* **16**, 1 (1986).
[2] J. W. Holt, M. Rho, and W. Weise, *Phys. Rep.* **621**, 2 (2016).
[3] G. Baym, T. Hatsuda, T. Kojo, P. D. Powell, Y. Song, and T. Takatsuka, *Rep. Prog. Phys.* **81**, 056902 (2018).
[4] Y. L. Ma and M. Rho, *Prog. Part. Nucl. Phys.* **113**, 103791 (2020).
[5] W.-G. Paeng, T. T. S. Kuo, H. K. Lee, and M. Rho, *Phys. Rev. C* **93**, 055203 (2016).
[6] W.-G. Paeng, T. T. S. Kuo, H. K. Lee, Y.-L. Ma, and M. Rho, *Phys. Rev. D* **96**, 014031 (2017).
[7] Y.-L. Ma and M. Rho, *Effective Field Theories for Nuclei and Compact-Star Matter* (World Scientific, Singapore, 2018).
[8] R. J. Crewther and L. C. Tunstall, *Phys. Rev. D* **91**, 034016 (2015).
[9] R. J. Crewther, *Universe* **6**, 96 (2020).
[10] M. Bando, T. Kugo, S. Uehara, K. Yamawaki, and T. Yanagida, *Phys. Rev. Lett.* **54**, 1215 (1985).
[11] M. Bando, T. Kugo, and K. Yamawaki, *Phys. Rep.* **164**, 217 (1988).
[12] M. Harada and K. Yamawaki, *Phys. Rep.* **381**, 1 (2003).
[13] J. D. Walecka, *Ann. Phys. (N.Y.)* **83**, 491 (1974).
[14] B. D. Serot and J. D. Walecka, *Int. J. Mod. Phys. E* **6**, 515 (1997).
[15] J. Boguta and A. R. Bodmer, *Nucl. Phys.* **A292**, 413 (1977).
[16] Y. Motohiro, Y. Kim, and M. Harada, *Phys. Rev. C* **92**, 025201 (2015); **95**, 059903(E) (2017).
[17] G. A. Lalazissis, J. Konig, and P. Ring, *Phys. Rev. C* **55**, 540 (1997).
[18] H. Mueller and B. D. Serot, *Nucl. Phys.* **A606**, 508 (1996).
[19] C. J. Horowitz and J. Piekarewicz, *Phys. Rev. Lett.* **86**, 5647 (2001).
[20] C. J. Horowitz and J. Piekarewicz, *Phys. Rev. C* **64**, 062802 (2001).
[21] S. Kubis and M. Kutschera, *Phys. Lett. B* **399**, 191 (1997).
[22] F. Hofmann, C. M. Keil, and H. Lenske, *Phys. Rev. C* **64**, 034314 (2001).
[23] B. Liu, V. Greco, V. Baran, M. Colonna, and M. Di Toro, *Phys. Rev. C* **65**, 045201 (2002).
[24] L. W. Chen, C. M. Ko, and B. A. Li, *Phys. Rev. C* **76**, 054316 (2007).
[25] N. Zabari, S. Kubis, and W. Wójcik, *Phys. Rev. C* **99**, 035209 (2019).
[26] N. Zabari, S. Kubis, and W. Wójcik, *Phys. Rev. C* **100**, 015808 (2019).
[27] T. Miyatsu, M.-K. Cheoun, and K. Saito, *Astrophys. J.* **929**, 82 (2022).
[28] F. Li, B. J. Cai, Y. Zhou, W. Z. Jiang, and L. W. Chen, *Astrophys. J.* **929**, 183 (2022).

- [29] F. E. Close and N. A. Tornqvist, *J. Phys. G* **28**, R249 (2002).
- [30] M. Napsuciale and S. Rodriguez, *Phys. Rev. D* **70**, 094043 (2004).
- [31] A. H. Fariborz, R. Jora, and J. Schechter, *Phys. Rev. D* **72**, 034001 (2005).
- [32] A. H. Fariborz, R. Jora, and J. Schechter, *Phys. Rev. D* **77**, 034006 (2008).
- [33] A. H. Fariborz, R. Jora, and J. Schechter, *Phys. Rev. D* **79**, 074014 (2009).
- [34] M. Harada, Scalar mesons in radiative decays and pi-pi scattering in *YITP Workshop on Multi-quark Hadrons: Four, Five and More?* (YITP-W-03-21) (2004), [arXiv: hep-ph/0408189](https://arxiv.org/abs/hep-ph/0408189).
- [35] A. H. Fariborz, R. Jora, J. Schechter, and M. N. Shahid, *Phys. Rev. D* **84**, 113004 (2011).
- [36] M. Harada, H. Hoshino, and Y. L. Ma, *Phys. Rev. D* **85**, 114027 (2012).
- [37] A. H. Fariborz, J. Schechter, S. Zarepour, and M. Zebarjad, *Phys. Rev. D* **90**, 033009 (2014).
- [38] L. Olbrich, Phenomenology of baryons in the extended linear sigma model, Master's thesis, Goethe U., Frankfurt (main), 2014.
- [39] L. Olbrich, M. Zétényi, F. Giacosa, and D. H. Rischke, *Phys. Rev. D* **93**, 034021 (2016).
- [40] D. Parganlija, P. Kovacs, G. Wolf, F. Giacosa, and D. H. Rischke, *Phys. Rev. D* **87**, 014011 (2013).
- [41] Y. Sugahara and H. Toki, *Nucl. Phys. A* **579**, 557 (1994).
- [42] H. Shen, H. Toki, K. Oyamatsu, and K. Sumiyoshi, *Nucl. Phys. A* **637**, 435 (1998).
- [43] D. Parganlija, F. Giacosa, and D. H. Rischke, *Phys. Rev. D* **82**, 054024 (2010).
- [44] C. Rosenzweig, J. Schechter, and C. G. Trahern, *Phys. Rev. D* **21**, 3388 (1980).
- [45] S. D. H. Hsu, F. Sannino, and J. Schechter, *Phys. Lett. B* **427**, 300 (1998).
- [46] D. Black, A. H. Fariborz, F. Sannino, and J. Schechter, *Phys. Rev. D* **59**, 074026 (1999).
- [47] R. L. Workman *et al.* (Particle Data Group), *Prog. Theor. Exp. Phys.* **2022**, 083C01 (2022).
- [48] A. Sedrakian, J. J. Li, and F. Weber, *Prog. Part. Nucl. Phys.* **131**, 104041 (2023).
- [49] J. M. Lattimer and Y. Lim, *Astrophys. J.* **771**, 51 (2013).
- [50] M. Farine, J. M. Pearson, and F. Tondeur, *Nucl. Phys. A* **615**, 135 (1997).
- [51] M. Dutra, O. Lourenco, J. S. Sa Martins, A. Delfino, J. R. Stone, and P. D. Stevenson, *Phys. Rev. C* **85**, 035201 (2012).
- [52] F. J. Fattoyev, C. J. Horowitz, J. Piekarewicz, and G. Shen, *Phys. Rev. C* **82**, 055803 (2010).
- [53] B. T. Reed, F. J. Fattoyev, C. J. Horowitz, and J. Piekarewicz, *Phys. Rev. Lett.* **126**, 172503 (2021).
- [54] B. P. Abbott *et al.* (LIGO Scientific and Virgo Collaborations), *Phys. Rev. Lett.* **121**, 161101 (2018).
- [55] Y. L. Ma and M. Rho, *Phys. Rev. D* **100**, 114003 (2019).
- [56] T. Zhao and J. M. Lattimer, *Phys. Rev. D* **102**, 023021 (2020).
- [57] J. I. Kapusta and T. Welle, *Phys. Rev. C* **104**, L012801 (2021).
- [58] J. Margueron, H. Hansen, P. Proust, and G. Chanfray, *Phys. Rev. C* **104**, 055803 (2021).
- [59] M. Hippert, E. S. Fraga, and J. Noronha, *Phys. Rev. D* **104**, 034011 (2021).
- [60] W. J. Xie and B. A. Li, *Astrophys. J.* **883**, 174 (2019).
- [61] S. Choi, T. Miyatsu, M.-K. Cheoun, and K. Saito, *Astrophys. J.* **909**, 156 (2021).
- [62] W.-G. Paeng, H. K. Lee, M. Rho, and C. Sasaki, *Phys. Rev. D* **88**, 105019 (2013).